Microelectronics Reliability 55 (2015) 407–410

Contents lists available at ScienceDirect

Microelectronics Reliability

journal homepage: www.elsevier.com/locate/microrel

Electron transport mechanism of tungsten trioxide powder thin film studied by investigating effect of annealing on resistivity

Wei Li [a,*], Akito Sasaki [b], Hideyuki Oozu [b], Katsuaki Aoki [b], Kuniyuki Kakushima [a], Yoshinori Kataoka [a], Akira Nishiyama [a], Nobuyuki Sugii [a], Hitoshi Wakabayashi [a], Kazuo Tsutsui [a], Kenji Natori [c], Hiroshi Iwai [a,c]

[a] Department of Electronics and Applied Physics, Interdisciplinary Graduate School of Science and Engineering, Tokyo Institute of Technology, 4259-S2-20 Nagatsuta-cho, Midori-ku, Yokohama, Kanagawa 226-8502, Japan
[b] Toshiba Material Co., LTD, 8, Shinsugita-Cho, Isogo-Ku, Yokohama 235-8522, Japan
[c] Frontier Research Center, Tokyo Institute of Technology, 4259-S2-20 Nagatsuta-cho, Midori-ku, Yokohama, Kanagawa 226-8502, Japan

ARTICLE INFO

Article history:
Received 2 September 2014
Received in revised form 22 October 2014
Accepted 23 October 2014
Available online 15 November 2014

Keywords:
Electron transport mechanism
Monoclinic tungsten trioxide powder thin film
Resistivity
Activation energy

ABSTRACT

We report a new approach for improving the recharging and discharging speed of lithium ion batteries based on understanding of the electron conduction mechanism of tungsten trioxide (WO_3) powder thin films fabricated from nanoparticles and used in lithium ion battery electrodes. Resistivity measurements are carried out after annealing in N_2 or 5% O_2 + 95% N_2 ambient. Annealing in N_2 ambient decreases the resistivity owing to the increased number of oxygen vacancies in the WO_3 thin film. Fitting results obtained from the resistivity are used to propose the simultaneous existence of two types of electron conduction mechanism, band conduction and nearest-neighbor hopping (NNH) conduction, contributing to electron conduction in WO_3 thin films.

1. Introduction

Transition-metal oxide materials are widely used as electrode materials in secondary lithium ion batteries owing to their high stability and high capacity for storing lithium ions [1,2]. Among the transition-metal oxide materials, WO_3 thin films, which are well known for their excellent ability to promote the reversible intercalation of lithium ions, are considered to be a possible cathode-active material for use in lithium ion rechargeable batteries [3]. Moreover, the porosity of WO_3 thin films makes it easier for lithium ions to undergo intercalation, leading to secondary lithium ion batteries with high energy density [4].

In the recharging and discharging processes of secondary lithium ion batteries, lithium ions are intercalated into or released from the cavities of a crystalline WO_3 thin film, while electrons simultaneously enter or leave the cavities of the film; thus, both lithium ion transportation and electron transportation affect the recharging and discharging speed [5]. Although the performance of lithium ion transportation has been extensively studied, detailed research on the mechanism of electron conduction in crystalline WO_3 thin films for their application as an active cathode is still required. Furthermore, to improve the recharging and discharging speed, it is necessary to develop processes that can increase the electron conductivity of crystalline WO_3 thin films. Two main types of WO_3 crystalline structure, i.e., monoclinic WO_3 (m-WO_3) and hexagonal WO_3 (h-WO_3), are usually chosen for the active cathode [6,7]. m-WO_3 is preferable owing to its stability even at high temperatures (above 400 °C) [8]. In this work, the electron transport mechanisms of m-WO_3 thin films formed from WO_3 nanoparticles were studied through measuring the film resistivity after annealing under various conditions. We clarified the impact of a high-temperature N_2 annealing process in improving electron conductivity and the dominant mechanisms contributing to the high conductivity of m-WO_3 thin films.

2. Experimental

An aqueous dispersion of WO_3 nanoparticles of about 30 nm diameter was sprayed on a SiO_2 substrate of 400 nm thickness, which was followed by annealing in air ambient at 450 °C for 30 min. Fig. 1(a) and (b) shows a transmission electron microscopy (TEM) image of the sample and electron diffraction patterns of points 1 and 2 in the TEM image, showing the crystalline structure respectively. Fig. 1(c) shows a typical X-ray diffraction spectrum of an m-WO_3 thin-film sample. The m-WO_3 thin film was formed

* Corresponding author. Tel.: +81 45 924 5847.
E-mail address: li.w.ad@m.titech.ac.jp (W. Li).

http://dx.doi.org/10.1016/j.microrel.2014.10.012
0026-2714/

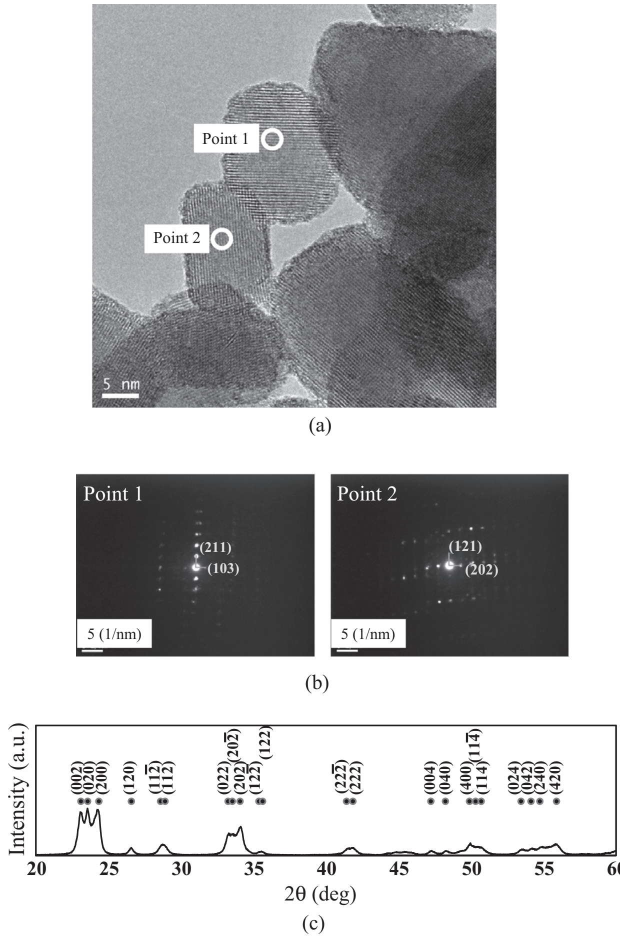

Fig. 1. (a) TEM image, (b) electron diffraction patterns, and (c) XRD spectrum of m-WO_3 formed from WO_3 nanoparticles and adopted in this study.

with a thickness of about 150 nm, a porosity of about 35%, and a Brunauer–Emmett–Teller (BET) specific surface area of about 37 m^2/g. The porosity of 35% was chosen for the experiment because, under this condition, a WO_3 film can be formed from WO_3 nanoparticles through a spraying method and the necking property of the nanoparticles can be obtained. When the porosity is less than 35%, a WO_3 coating cannot be formed. When the porosity is more than 35%, the resistivity of WO_3 increases. The TEM image also reveals that nanoparticles are necked with each other, which improves the conductivity of the obtained m-WO_3 thin film [9].

The four-point probe method was used to measure the resistivity with tungsten metal deposited by RF magnetron sputtering used for the electrodes. Tungsten electrode patterns were formed by the wet etching method with H_2O_2 solution. The formed sample was annealed at various temperatures in N_2 or 5% O_2 + 95% N_2 ambient. Then the resistivity was measured in the temperature range of 243–443 K.

3. Results

Fig. 2 shows the measured resistivity (plotted against $1000/T$) for three samples, which were not subjected to annealing, annealed in N_2 ambient at 300 °C for 5 min, and annealed in N_2 ambient at 300 °C for 5 min followed by 5% O_2 + 95% N_2 ambient at 300 °C for 5 min. Although annealing in N_2 reduces the resistivity of the m-WO_3 film, subsequent annealing in 5% O_2 + 95% N_2 ambient results in the resistivity returning to its initial value.

Activation energy (E_a) values were derived for the three samples and are shown in Table 1, where E_a is the minimum energy required for a chemical reaction and can be interpreted in the form of a trap depth in the bandgap in this study. The calculation method is following the relation in Eq. (1) [10]:

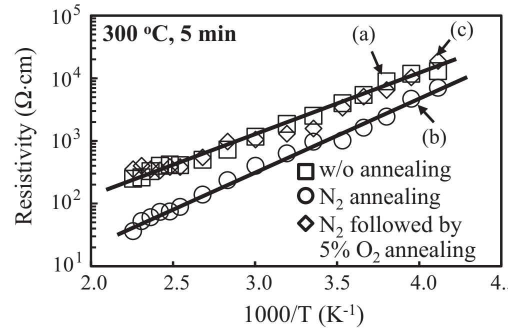

Fig. 2. Measured resistivity ρ versus $1000/T$ for samples annealed in different ambients: no annealing (a), annealed in N_2 ambient at 300 °C for 5 min (b), annealed in N_2 ambient at 300 °C for 5 min followed by 5% O_2 + 95% N_2 ambient at 300 °C for 5 min.

$$\rho = \rho_0 \exp(E_a/kT) \Rightarrow \ln \rho = \frac{E_a}{k} \cdot \frac{1}{T} + \ln \rho_0 \quad (1)$$

Here, ρ is the measured resistivity, ρ is a pre-exponential factor, T is the measurement temperature, which is from 443 K to 243 K in this study, and k is the Boltzmann constant. E_a is proportional to the gradient of the resistivity-temperature curves shown in Fig. 2.

Fig. 3 shows the resistivity ρ plotted against $1000/T$ for the samples after annealing in N_2 at temperatures from 300 °C to 750 °C for 5 min. For the samples annealed at temperatures from 300 °C to 500 °C, the gradients of the curves were almost the same as that for the sample without annealing. On the other hand, for the samples annealed at temperatures from 600 °C to 750 °C, the curves could be divided into two parts with different gradients. The first part is in the temperature range from 443 K to 393 K, which has almost the same gradient as that for the sample without annealing. The other part is in the temperature range from 373 K to 243 K, which has a smaller gradient.

4. Discussion

The changes in the resistivity after annealing in N_2 or 5% O_2 + 95% N_2 ambient exhibited in Fig. 2 can be explained by oxygen vacancy generation and annihilation in a tungsten oxide thin film. After annealing at 300 °C in N_2 ambient, oxygen vacancies, which create trap levels in the bandgap for activated electrons to mobile, were generated, leading to a decrease in the resistivity. After annealing at 300 °C in 5% O_2 + 95% N_2 ambient, the oxygen vacancies were annihilated, leading to a decrease in the number of carrier trap sites and a simultaneous decrease in the number of carriers taking part in the conduction. Therefore, the resistivity increased to almost the same value as before annealing. Moreover, the E_a values shown in Table 1 were approximately 0.2 eV, indicating that oxygen vacancies stably exist at approximately 0.2 eV below the bottom of the conduction band.

In Fig. 3, which is based on the method used to obtain E_a mentioned above, the obtained gradients are proportional to the activation energy E_a. Normally, for semiconductor materials, there

Table 1
Derived values of E_a for different annealing conditions.

	w/o Annealing	300 °C Annealing in N_2 ambient	300 °C Annealing in 5% O_2 ambient
E_a (eV)	0.19	0.23	0.18